



HAL
open science

ON THE AUTOXIDATION OF TERPENES: DETECTION OF OXYGENATED AND AROMATIC PRODUCTS

Zahraa Dbouk, Nesrine Belhadj, Maxence Lailliau, Roland Benoit, Philippe
Dagaut

► **To cite this version:**

Zahraa Dbouk, Nesrine Belhadj, Maxence Lailliau, Roland Benoit, Philippe Dagaut. ON THE AUTOXIDATION OF TERPENES: DETECTION OF OXYGENATED AND AROMATIC PRODUCTS. 15th International Conference on Combustion Technologies for a Clean Environment, Jun 2022, Lisbon (Portugal), Portugal. hal-04385272

HAL Id: hal-04385272

<https://univ-orleans.hal.science/hal-04385272v1>

Submitted on 10 Jan 2024

HAL is a multi-disciplinary open access archive for the deposit and dissemination of scientific research documents, whether they are published or not. The documents may come from teaching and research institutions in France or abroad, or from public or private research centers.

L'archive ouverte pluridisciplinaire **HAL**, est destinée au dépôt et à la diffusion de documents scientifiques de niveau recherche, publiés ou non, émanant des établissements d'enseignement et de recherche français ou étrangers, des laboratoires publics ou privés.

Public Domain

ON THE AUTOXIDATION OF TERPENES: DETECTION OF OXYGENATED AND AROMATIC PRODUCTS

Zahraa Dbouk^{a,b}, Nesrine Belhadj^{a,b}, Maxence Lailliau^{a,b}, Roland Benoit^a, Philippe Dagaut^a

^a C.N.R.S., 1C Avenue de la Recherche Scientifique, Orléans, 45071, France

^b Université d'Orléans, Avenue de Parc Floral, Orléans, 45067, France

ABSTRACT

Limonene-O₂-N₂ and α -pinene-O₂-N₂ mixtures were oxidized in a jet-stirred reactor at atmospheric pressure, in the cool flame regime, and fuel-lean conditions. Samples of the reacting mixtures were collected, dissolved in acetonitrile, and analyzed by Orbitrap mass spectrometry after flow injection or chromatographic separation by ultra-high-performance liquid chromatography and +/- heated electrospray ionization and +/- atmospheric pressure chemical ionization. OH/OD exchange using D₂O and reaction with 2,4-dinitrophenylhydrazine were carried out for probing the existence of hydroxy, hydroperoxy, and carbonyl functions in the products, respectively. A huge set of products of oxidation, including highly oxygenated organic products with five and more oxygen atoms, was observed. Aromatic and polyunsaturated products were detected. Van Krevelen plots, computed oxidation state of carbon and degree of unsaturation in products were used to rationalize the results.

Keywords: monoterpenes, oxidation, pollutants, jet-stirred reactor, Orbitrap

1. INTRODUCTION

Terpenes are naturally released by vegetation. They constitute a large fraction of volatile organic chemicals detected in the troposphere [1]. Besides, because of their high-energy-density, they could be used as biojet fuels [2]. Monoterpenes show cetane numbers of the order of 20. Then, one could also use them as drop-in fuels to reduce carbon footprint in transportation. However, the use of terpenes as biofuel or drop-in fuel would certainly contribute to increasing their concentration in the troposphere through unburnt fuel emissions and evaporation during transport and refueling. While terpenes kinetics of oxidation under atmosphere-relevant conditions has been the topic of many works, a good understanding of the multiple oxidation routes has not been attained yet [3]. The chemical kinetics of combustion of such chemicals has not received much attention to date since only burning velocity in air and impact on ignition have been reported [4, 5]. In hydrocarbons (RH) combustion we consider the production of oxygenates such as ketohydroperoxides (KHPs) which lead to chain branching via decomposition [6]: $\text{RH} + \cdot\text{OH} \rightarrow \text{R} \cdot + \text{H}_2\text{O}$ (1), $\text{R} \cdot + \text{O}_2 \rightleftharpoons \text{RO}_2 \cdot$ (2), $\text{RO}_2 \cdot + \text{HO}_2 \cdot \rightleftharpoons \text{RO}_2\text{H} + \text{O}_2$ (3), $\text{RO}_2 \cdot + \text{RH} \rightleftharpoons \text{RO}_2\text{H} + \text{R} \cdot$ (4), $\text{RO}_2 \cdot \rightleftharpoons \cdot\text{QO}_2\text{H}$ (5), $\text{RO}_2 \cdot \rightleftharpoons \text{Q}$ (unsaturated product) + $\text{HO}_2 \cdot$ (6),

$\cdot\text{QO}_2\text{H} \rightleftharpoons \cdot\text{OH} + \text{QO}$ (cyclic ether) (7), $\cdot\text{QO}_2\text{H} + \text{O}_2 \rightleftharpoons \cdot\text{OOQO}_2\text{H}$ (8), $\cdot\text{O}_2\text{QO}_2\text{H} \rightleftharpoons \text{HO}_2 \cdot \text{PO}_2\text{H}$ (9), $\text{HO}_2 \cdot \text{PO}_2\text{H} \rightleftharpoons \cdot\text{OH} + \text{HO}_2\text{P}=\text{O}$ (KHPs) (10), $\text{HO}_2\text{P}=\text{O} \rightleftharpoons \cdot\text{OH} + \text{OP} \cdot \text{O}$ (11). Besides, the formation of more oxygenated products in cool flames of a large range of fuels has been reported in recent studies [7, 8]. There, alternative oxidation pathways proceed via an internal H-transfer in the $\cdot\text{O}_2\text{QO}_2\text{H}$ intermediate involving a H-C group other than the H-COOH group responsible for KHPs formation. It opens new oxidation pathways including a third O₂ addition to $\text{HO}_2\text{PO}_2\text{H}$ yielding $\cdot\text{O}_2\text{P}(\text{O}_2\text{H})_2$. Such sequence of H-transfer and O₂ addition can repeat several times, yielding highly oxidized products. Besides, $\cdot\text{QO}_2\text{H}$ decomposition yields stable products and radicals via Reaction (7), $\cdot\text{QO}_2\text{H} \rightarrow \text{olefin} + \text{carbonyl} + \cdot\text{OH}$ (12), and $\cdot\text{QO}_2\text{H} \rightarrow \text{HO}_2 \cdot + \text{olefin}$ (13). In the case of unsaturated reactants, the Waddington mechanism [9] can proceed. It starts by an $\cdot\text{OH}$ addition on a C=C double bonds and continues by O₂ addition and H-atom internal transfer from the -OH group to the -OO \cdot peroxy group, and decomposition: $\text{R}^1\text{-C}=\text{C}-\text{R}^2 + \cdot\text{OH} \rightleftharpoons \text{R}^1\text{-}\dot{\text{C}}\text{-C}(\text{-R}^2)\text{-OH}$ (14), $\text{C}(\text{-R}^1)\text{-C}(\text{-R}^2)\text{-OH} + \text{O}_2 \rightleftharpoons \cdot\text{OO-C}(\text{-R}^1)\text{-C}(\text{-R}^2)\text{-OH}$ (15), $\cdot\text{OO-C}(\text{-R}^1)\text{-C}(\text{-R}^2)\text{-OH} \rightleftharpoons \text{HOO-C}(\text{-R}^1)\text{-C}(\text{-R}^2)\text{-O} \cdot$ (16), $\text{HOO-C}(\text{-R}^1)\text{-C}(\text{-R}^2)\text{-O} \cdot \rightarrow \text{R}^1\text{-C}=\text{O} + \text{R}^2\text{-C}=\text{O} + \cdot\text{OH}$ (17). Via this sequence of reactions, the hydroxy radical initially consumed in

*Corresponding author email: philippe.dagaut@cnrs-orleans.fr

Reaction (14) is finally regenerated in Reaction (17). The Korcek mechanism [9] can also occur. It transforms γ -keto hydroperoxides into a carbonyl and a carboxylic acid. The Korcek mechanism has been considered in recent combustion models [10, 11]. Besides, the potential formation of aromatic products from the oxidation of monoterpenes has not received attention.

The present work aims to better characterize the autoxidation products of two terpenes, limonene and a α -pinene, under cool-flame conditions and investigate the formation of aromatics there. To this end, we carried out oxidation experiments in a jet-stirred reactor at 1 bar, and oxidation products were characterized using high-resolution mass spectrometry.

2. EXPERIMENT

2.1 Oxidation experiments

Experiments were conducted in a 42 mL fused silica jet-stirred-reactor (JSR) introduced earlier [12]. As previously [13, 14] for the injection of the fuels, we used a HPLC pump with an online degasser. The fuels were delivered to a vaporizer assembly fed with a flow of N_2 . Fuel- N_2 and O_2 - N_2 flowed separately to the JSR to avoid oxidation before reaching the reactor. The flow rates of N_2 and O_2 were delivered by mass flow meters. Thermocouples (0.1 mm Pt-Pt/Rh-10% wires protected by a thin silica tube) were moved along the vertical axis of the JSR to check thermal homogeneity (gradients of < 1 K/cm). To study the oxidation of the fuels in the cool-flame regime (520–680 K), we used 1% of fuel and operated at 1 bar, in fuel-lean conditions ($\phi = 0.5$), and 1.5 s of mean residence time.

2.1 Chemical analyses

Low-temperature oxidation products were dissolved into 20 mL of ≥ 99.9 pure acetonitrile, maintained at 273 K, through 60 min bubbling. They were stored in a freezer at 258 K for next chemical analyses. Flow injection analyses/heated electrospray ionization (FIA/HESI) were done. The samples were analyzed by Orbitrap Q-Exactive (high-resolution mass spectrometry, HRMS). We performed mass calibrations in positive and negative modes by injecting \pm -HESI calibration mixtures. Reverse-phase ultra-high-performance liquid chromatography (RP-UHPLC) analyses were conducted using a C18 analytical column (Phenomenex Luna, 1.6 μ m, 100 \AA , 100x2.1 mm). 3 μ L of samples were eluted by water-acetonitrile (ACN) mix at a flow rate of 250 μ L/min (gradient 5% to 90% ACN, during 33 min). Also, atmospheric pressure chemical ionization (APCI) was used in positive and negative modes. For determining the chemical structure of oxidation products after RP-UHPLC separation, MS/MS analyses were performed using the lowest collision cell energy (10 eV). As in preceding works [13, 14] 2,4-Dinitrophenylhydrazine (2,4-DNPH) addition to samples was also used to assess the presence of carbonyl compounds. As before [7, 13–15], to evaluate to the existence of a hydroxyl ($-\text{OH}$) or

hydroperoxyl ($-\text{OOH}$) groups in oxidation products, we performed OH/OD exchange by addition of D_2O to the samples. We analyzed these solutions by FIA-HESI-HRMS and RP-UHPLC-APCI-HRMS.

3. RESULTS AND DISCUSSION

Many oxidation products were detected during the oxidation of the two terpenes. Oxidation products, containing \geq O-atoms, were detected: $C_7H_{10}O_{4,5}$, $C_8H_{12}O_{2,4}$, $C_8H_{14}O_{2,4}$, $C_9H_{12}O$, $C_9H_{14}O_{1,3-5}$, $C_{10}H_{12}O_2$, $C_{10}H_{14}O_{1-9}$, $C_{10}H_{16}O_{2-5}$, and $C_{10}H_{18}O_6$. Figure 1 shows results obtained for KHPs and isomers and for diketones which result from KHPs decomposition. As can be seen from that figure, both products peak at a temperature ~ 620 K. Carbonyl compounds from the Waddington mechanism on *exo*- and *endo*-double bonds ($C=C$) of limonene were observed as well as products of their oxidation. They are not presented here, due to space limitations.

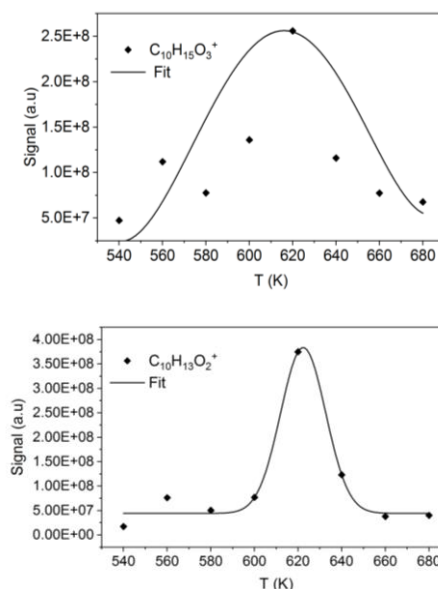


Figure 1: Products of oxidation of limonene obtained by HRMS (symbols). The data for KHPs and isomers (top, $C_{10}H_{14}O_3$) and diketones and isomers (bottom, $C_{10}H_{12}O_2$) were obtained by FIA and HESI (+), i.e., $C_{10}H_{15}O_3^+$ m/z 183.1015 and $C_{10}H_{13}O_2^+$ m/z 165.0910, respectively.

Earlier, it was reported [16] a higher reactivity of the *endo* double bond vs. the *exo* double bond. In line with that result, higher ion signal was recorded for isoprenyl-6-oxoheptanal ($C_{10}H_{17}O_2^+$) than for limonaketone ($C_9H_{15}O^+$), which result from oxidation of *endo* and *exo* double bonds, respectively. Products of the Korcek mechanism (carboxylic acids and carbonyls) were also detected. Among the 18 KHPs deriving from limonene oxidation, four isomers could decompose via the Korcek mechanism. But, only one isomer can possibly yield a cyclic intermediate peroxide linking the carbonyl and OOH groups which yields a carbonyl compound, $C_9H_{12}O$, and formic acid, CH_2O_2 by

decomposition (Fig. 2). Both products were detected by UHPLC-HRMS in this study.

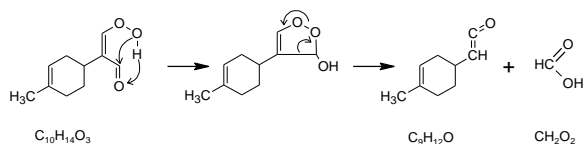


Figure 2: Korcek mechanism during limonene oxidation.

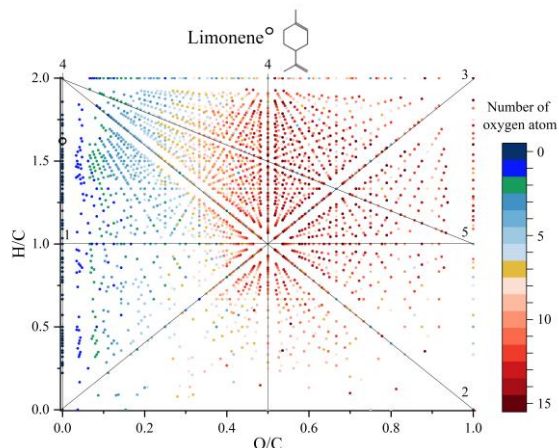


Figure 3: Van Krevelen plot for limonene oxidation products. (sample taken at 640 K). Lines indicate 1: oxidation, 2: carbonylation, 3: hydration, 4: dehydrogenation, 5: carboxylation, or reverse processes [17].

The formation of C_nH_2 , C_nH_4 , and C_nH_6 ($n \geq 4$) isomers was observed for both terpene fuels on line 4 with $O/C = 0$ in Van Krevelen plots using HESI+/- FIA-HRMS data (Figs. 3-4; the position of the fuels is shown as a circle). These plots indicated the formation of aromatics ($H/C < 0.7$ and $O/C = 0$) and polyunsaturated products. In the space defined by $0 < O/C < 0.2$, we observed products of oxidation (line 1) and dehydrogenation (line 4). For $H/C < 1$, the degree of oxidation of products is less than for $H/C > 1$. Plotting the percentage of unsaturation versus the number of carbon atoms in the detected products (Fig. 5) confirms that high degrees of unsaturation are reached and the products mass range extends over m/z 550.

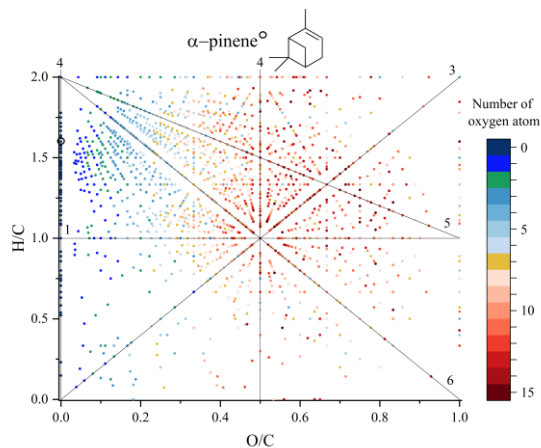


Figure 4: Van Krevelen plot for α -pinene oxidation products. HESI+/-, FIA-HRMS (sample taken at 640 K).

The degree of unsaturation is defined as: $(3 \times C + 1) / (C - H/2 + 1)$ where H and C represent the number of hydrogen and C-atoms, respectively.

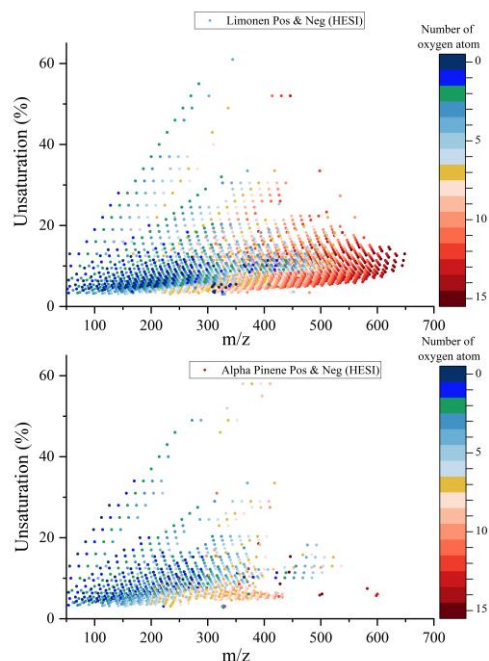


Figure 5: Variation of the degree of unsaturation in the oxidation products of limonene (top) and α -pinene (bottom).

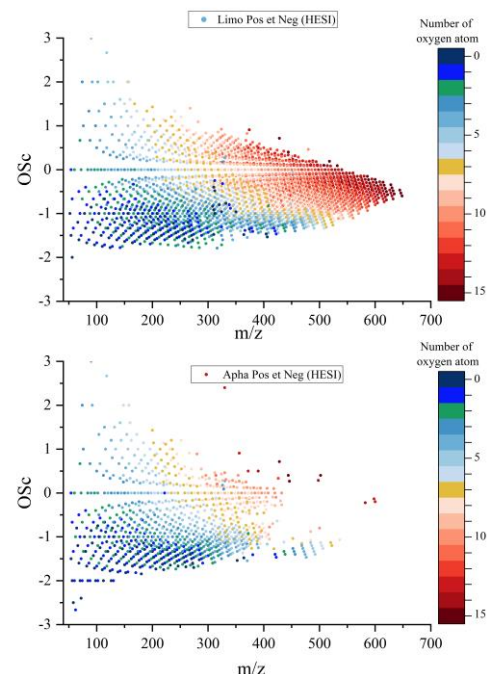


Figure 6: Overview of the distribution of limonene (top) and α -pinene (bottom) oxidation products observed (+/- HESI) by plotting OSc versus carbon number in detected chemical formulae. $OSc \approx 2 O/C - H/C$ [18] where H , C , and O represent the number of hydrogen, carbon, and oxygen atoms, respectively.

Below m/z 550, similar trends are observed, although the data show significantly more products with high m/z in the case of limonene, which could be due to the presence of both *endo* and *exo* C=C in limonene. These data were obtained under the following conditions: HESI+/-, FIA-HRMS (sample taken at 640 K). Whereas the presently observed formation of aromatics and polyunsaturated products under cool-flame conditions was rather unexpected, it should be investigated further under simulated atmospheric oxidation conditions since the oxidation of aromatics could significantly contribute to the formation of secondary organic aerosols. The oxidation state of carbon (OSc) in products was also studied (Fig. 6). Besides the fact that higher m/z oxidation products were detected in limonene oxidation samples, similar trends were observed for both fuels.

4. CONCLUSIONS

In this study we detected a large set of complex products of oxidation formed from cool flames of two monoterpenes, limonene and α -pinene, at atmospheric pressure and fuel-lean conditions. Oxidation pathways including autoxidation, the Waddington mechanism involving *exo*- and *endo*-double bonds (C=C), autoxidation of its products, and the Korcek mechanism. The formation of aromatic and polyunsaturated products was observed during the autoxidation of the two fuels. The oxidation of limonene under the present conditions forms significantly more high molecular weight products. This work demonstrates that oxidation pathways are numerous and complex and many complex chemical products can be formed. The oxidation products detected in this work can be emitted to the troposphere, which would increase the concentration of VOCs contributing to the formation of particulates.

ACKNOWLEDGMENTS

Financial support from CPER and EFRD (PROMESTOCK and APPROPOR-e projects), the French Ministry of Research (MESRI), the Labex CAPRYSES (ANR-11-LABX-0006) and the Labex VOLTAIRE (ANR-10-LABX-100) is gratefully acknowledged.

5. REFERENCES

- [1] J. H. Seinfeld; S. N. Pandis, *Atmospheric Chemistry and Physics: From Air Pollution to Climate Change*, Wiley-Interscience, Hoboken, NJ, 2006, pp. 1-1232.
- [2] M. Pourbafrani; G. Forgács; I. S. Horváth; C. Niklasson; M. J. Taherzadeh, Production of biofuels, limonene and pectin from citrus wastes, *Bioresour. Technol.* 101 (2010) 4246-4250.
- [3] T. Berndt; S. Richters; R. Kaethner; J. Voigtländer; F. Stratmann; M. Sipilä; M. Kulmala; H. Herrmann, Gas-Phase Ozonolysis of Cycloalkenes: Formation of Highly Oxidized RO2 Radicals and Their Reactions with NO, NO2, SO2, and Other RO2 Radicals, *The Journal of Physical Chemistry A* 119 (2015) 10336-10348.
- [4] K. Chetehouna; L. Courty; C. Mounaim-Rousselle; F. Halter; J.-P. Garo, Combustion Characteristics of p-Cymene Possibly Involved in Accelerating Forest Fires, *Combust. Sci. Technol.* 185 (2013) 1295-1305.
- [5] L. Courty; K. Chetehouna; F. Halter; F. Foucher; J. P. Garo; C. Mounaim-Rousselle, Experimental determination of emission and laminar burning speeds of alpha-pinene, *Combust. Flame* 159 (2012) 1385-1392.
- [6] C. Morley, A Fundamentally Based Correlation Between Alkane Structure and Octane Number, *Combust. Sci. Technol.* 55 (1987) 115-123.
- [7] Z. Wang; D. M. Popolan-Vaida; B. Chen; K. Moshhammer; S. Y. Mohamed; H. Wang; S. Sioud; M. A. Raji; K. Kohse-Höinghaus; N. Hansen; P. Dagaut; S. R. Leone; S. M. Sarathy, Unraveling the structure and chemical mechanisms of highly oxygenated intermediates in oxidation of organic compounds, *Proceedings of the National Academy of Sciences* 114 (2017) 13102-13107.
- [8] Z. D. Wang; B. J. Chen; K. Moshhammer; D. M. Popolan-Vaida; S. Sioud; V. S. B. Shankar; D. Vuilleumier; T. Tao; L. Ruwe; E. Brauer; N. Hansen; P. Dagaut; K. Kohse-Hoinghaus; M. A. Raji; S. M. Sarathy, n-Heptane cool flame chemistry: Unraveling intermediate species measured in a stirred reactor and motored engine, *Combust. Flame* 187 (2018) 199-216.
- [9] D. J. M. Ray; A. Redfearn; D. J. Waddington, Gas-phase oxidation of alkenes: decomposition of hydroxy-substituted peroxy radicals, *Journal of the Chemical Society, Perkin Transactions 2* (1973) 540-543.
- [10] E. Ranzi; C. Cavallotti; A. Cuoci; A. Frassoldati; M. Pelucchi; T. Faravelli, New reaction classes in the kinetic modeling of low temperature oxidation of n-alkanes, *Combust. Flame* 162 (2015) 1679-1691.
- [11] C. Xie; M. Lailliau; G. Issayev; Q. Xu; W. Chen; P. Dagaut; A. Farooq; S. M. Sarathy; L. Wei; Z. Wang, Revisiting low temperature oxidation chemistry of n-heptane, *Combust. Flame* 242 (2022) 112177.
- [12] P. Dagaut; M. Cathonnet; J. P. Rouan; R. Foulatier; A. Quilgars; J. C. Boettner; F. Gaillard; H. James, A jet-stirred reactor for kinetic studies of homogeneous gas-phase reactions at pressures up to ten atmospheres (≈ 1 MPa), *Journal of Physics E: Scientific Instruments* 19 (1986) 207-209.
- [13] N. Belhadj; R. Benoit; P. Dagaut; M. Lailliau; Z. Serinyel; G. Dayma, Oxidation of di-n-propyl ether: Characterization of low-temperature products, *Proc. Combust. Inst.* 38 (2021) 337-344.
- [14] N. Belhadj; M. Lailliau; R. Benoit; P. Dagaut, Towards a Comprehensive Characterization of the Low-Temperature Autoxidation of Di-n-Butyl Ether, *Molecules* 26 (2021) 7174.
- [15] N. Belhadj; R. Benoit; P. Dagaut; M. Lailliau, Experimental characterization of n-heptane low-temperature oxidation products including keto-hydroperoxides and highly oxygenated organic molecules (HOMs), *Combust. Flame* 224 (2021) 83-93.
- [16] B. Witkowski; M. Al-sharafi; T. Gierczak, Kinetics of Limonene Secondary Organic Aerosol Oxidation in the Aqueous Phase, *Environmental Science & Technology* 52 (2018) 11583-11590.
- [17] S. Kim; R. W. Kramer; P. G. Hatcher, Graphical Method for Analysis of Ultrahigh-Resolution Broadband Mass Spectra of Natural Organic Matter, the Van Krevelen Diagram, *Anal. Chem.* 75 (2003) 5336-5344.
- [18] J. H. Kroll; N. M. Donahue; J. L. Jimenez; S. H. Kessler; M. R. Canagaratna; K. R. Wilson; K. E. Altieri; L. R. Mazzoleni; A. S. Wozniak; H. Bluhm; E. R. Mysak; J. D. Smith; C. E. Kolb; D. R. Worsnop, Carbon oxidation state as a metric for describing the chemistry of atmospheric organic aerosol, *Nature Chemistry* 3 (2011) 133-139.